

# Study the $J_{SC}$ loss of full area SHJ solar cells caused by edge recombination

Cite as: J. Renewable Sustainable Energy **11**, 023503 (2019); doi: 10.1063/1.5085045

Submitted: 8 December 2018 · Accepted: 29 March 2019 ·

Published Online: 16 April 2019



View Online



Export Citation



CrossMark

Xingbing Li, Lifei Yang,<sup>a)</sup> Wenbin Zhang, and Qi Wang

## AFFILIATIONS

GCL System Integration Technology Co., Ltd., Suzhou 215000, China

<sup>a)</sup>E-mail: ylf02@126.com

## ABSTRACT

We have demonstrated that the edge recombination effect exists in full area industrial silicon heterojunction (SHJ) solar cells, which can cause significant short-circuit current density ( $J_{SC}$ ) loss. The mechanism behind this observation was studied using different SHJ cell structures. We demonstrated further that this  $J_{SC}$  loss effect can be suppressed effectively by simply controlling the gap between the edge of the transparent conductive oxide layer and that of the cell. Using this strategy, the average  $J_{SC}$  of our state-of-art SHJ solar cells was enhanced by 0.36 mA/cm<sup>2</sup>, resulting in an average efficiency gain of 0.28% absolute.

Published under license by AIP Publishing. <https://doi.org/10.1063/1.5085045>

## I. INTRODUCTION

The impact of edge recombination on homojunction silicon solar cells has long been studied.<sup>1–4</sup> It has been demonstrated that the edge recombination increases the nonideal dark saturation current  $J_{02}$  of the solar cell, leading to reduced fill factor ( $FF$ ) and open-circuit voltage ( $V_{OC}$ ), and therefore causes significant efficiency loss both for small area solar cells<sup>5,6</sup> and full area industrial solar cells.<sup>7</sup>

Silicon heterojunction (SHJ) solar cells have gained much attention in recent years because of their high efficiency, small temperature coefficient, and simple fabrication process.<sup>8–10</sup> For this type of solar cell, the highest efficiency of 25.1% was measured through a shadow mask with an aperture area of 151.9 cm<sup>2</sup> on a 6-in. SHJ solar cell.<sup>11</sup> This indicates that the efficiency of the full area 6-in. SHJ solar cell should be lower, and there is an efficiency loss at the edge of the cell.

In this work, we found that the edge recombination loss effect indeed exists in full area SHJ solar cells, which can not only lead to reduced  $FF$ , but also cause a pronounced decrease in  $J_{SC}$ . The mechanism behind this observation was studied using designed SHJ cell structures, based on which we demonstrated that the  $J_{SC}$  loss at the cell edge can be suppressed effectively by simply controlling the gap between the edge of the transparent conductive oxide (TCO) layer and that of the cell. Using this strategy, the average  $J_{SC}$  of our SHJ solar cells was increased by 0.36 mA/cm<sup>2</sup>, resulting in an average efficiency gain of 0.28% absolute.

## II. EXPERIMENTS

The 6 in. (156 × 156 mm<sup>2</sup>) n-type c-Si (100) wafers with a resistivity of 3–4 Ω cm were used as substrates. A wet-chemical process

with an alkaline solution was applied to remove saw damage and create a random pyramid surface texture. The final wafer thickness was approximately 145 μm. The textured wafers were then cleaned with a standard wet-chemical cleaning sequence RCA (Radio Corporation of America) 1 and 2, followed by a dip in dilute HF (1%) to remove the oxide film. The intrinsic amorphous silicon (i-a-Si:H) and doped amorphous silicon (p-a-Si:H and n-a-Si:H) stack layers were deposited on both side of the wafer via HWCVD (hot wire CVD) technology. Then, ~80 nm TCO layers on both sides were deposited by magnetron sputtering method. A gap between the edge of the TCO layer on a p-a-Si:H or n-a-Si:H side and the edge of the cell is designed to avoid edge shunting. Finally, silver electrodes on both sides were formed by screen-printing low-temperature silver paste and then curing at 200 °C for 30 min. The photoluminescence lifetime mapping of the SHJ solar cell without metallization but undergoing an annealing treatment at 200 °C for 30 min was measured by using a Luminescence Inspection System (BT imaging, LIS-R3). The external quantum efficiency (EQE) and internal quantum efficiency (IQE) spectra of the SHJ solar cells were determined using a quantum efficiency-reflection system (Industrial Vision Technology, PVE300), while the current density-voltage ( $J$ - $V$ ) characteristics of the SHJ solar cells were measured under standard test conditions with a solar cell  $I$ - $V$  tester (Industrial Vision Technology, VS-6820) equipped with a class AAA solar simulator.

## III. RESULTS AND DISCUSSION

Figure 1(b) shows the variation of the photovoltaic parameters with the illumination area measured on a SHJ solar cell [see Fig. 1(a)].

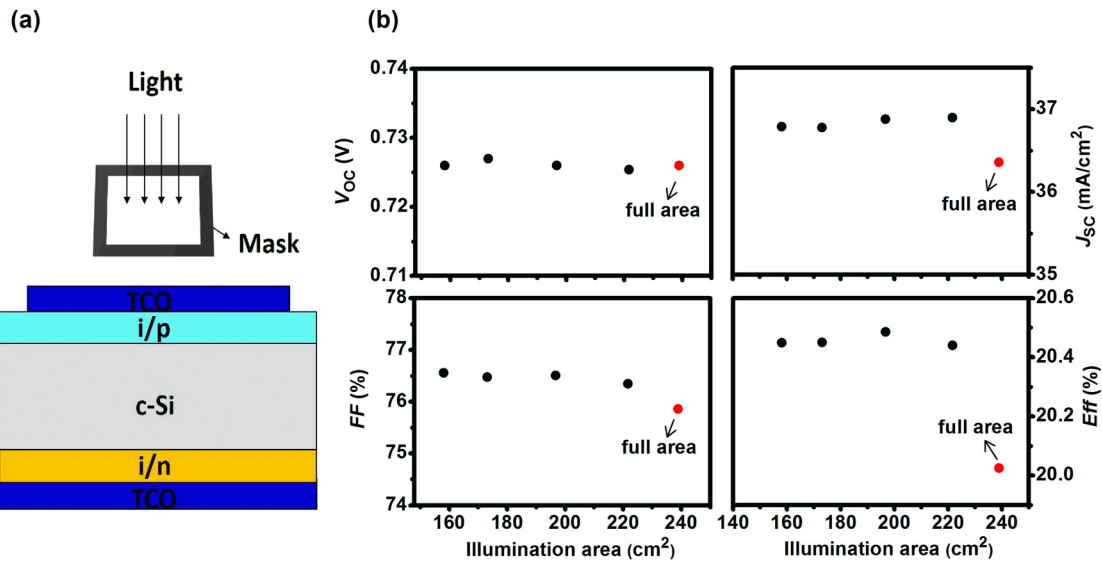


**FIG. 1.** (a) Schematic diagram showing the structure of a SHJ solar cell, in which i/p represents the i-a-Si:H/p-a-Si:H stack layer and i/n represents the i-a-Si:H/n-a-Si:H stack layer. Shadow masks were applied for efficiency measurement, except for the full area solar cell, to study the (b) variation of the photovoltaic parameters ( $V_{oc}$ ,  $J_{sc}$ , FF, and Eff) of the cell with a defined illumination area.

Note that the illumination area is defined by shadow masks made of black paper, which completely cover the rest of the area of the SHJ solar cell leaving only the area inside the shadow mask as the illumination area. It can be observed that there is no clear relationship between the  $V_{oc}$  and the illumination area, while the FF decreases slightly with the illumination area, which should be related to the increased silver electrode resistance for a larger illumination area. Note that the FF decrease is more pronounced when measuring the full area SHJ solar cell, which we believe is caused by the edge recombination effect similar to that of the homojunction silicon solar cells. From a fundamental point of view, there is a disrupter of the crystal lattice at the cell edge that exposes a defect-rich surface, but unlike the front and rear surfaces, the edges are normally poorly passivated thus causing edge recombination. For the case of an exposed p-n junction bordering the cell edge, like in the full area SHJ solar cell, it is found that the edge recombination in the space charge region (SCR) can result in an injection-level-dependent lifetime in silicon (i.e., reduced effective carrier lifetime at a low injection level)<sup>12,13</sup> as well as an increasing nonideal dark saturation current  $J_{02}$  of the solar cell. This will result in reduced FF (by lowering pseudo FF) and  $V_{oc}$ , as reported by the previous study on the homojunction silicon solar cells.<sup>1,3,14</sup> For the SHJ solar cells that commonly feature very low device recombination, FF is more sensitive to the injection-level-dependent lifetime effect than  $V_{oc}$  because the silicon absorbers indeed operate in high-injection in open-circuit, which is limited by Auger recombination.<sup>11,15</sup> This explains the above observation that a clear FF loss due to edge recombination is observed, whereas no significant change in  $V_{oc}$  is found. The largest variation, however, comes from the  $J_{sc}$  when measuring the full area SHJ solar cell. It can be found that a  $J_{sc}$  reduction of about 0.5 mA/cm² results in a cell efficiency decrease closer to 0.5% absolute. This observation clearly shows a  $J_{sc}$  loss at the cell edge of the full area SHJ solar cell.

Figures 2(a) and 2(b) show the external quantum efficiency (EQE) and internal quantum efficiency (IQE) curves of the SHJ solar

cell measured at the cell center (curves A), the cell edge within TCO covering (curves B) and the cell edge beyond TCO covering (curves C), respectively. Note that the area of the light spot of the EQE measurement is  $0.7 \times 5 \text{ mm}^2$  [see Fig. 2(c)], which is convenient to differ between A, B, and C. It can be found that the quantum efficiency (QE) responses decay in the vicinity of the cell edge, which means  $J_{sc}$  loss at the edge of the solar cell. As shown in Fig. 2(d), there are black edge regions with various widths from 2 mm to 9 mm in the PL image of the SHJ solar cell, indicating a reduced lifetime near the cell edge. The reduction of QE responses seen in Fig. 2(c) thus owes to the loss of light generated carriers near the cell edge which is consistent with the observation of Fig. 2(d). It is well known that the SHJ solar cell features a high quality a-Si:H/c-Si interface, which is sensitive to the processes of wafer cleaning, wafer transfer, and the a-Si:H passivation property. We believe that the low lifetime area near the cell edge is a consequence of edge recombination due to insufficient a-Si:H passivation of the cell edge. The localized low lifetime points [black spots in Fig. 2(d)], in contrast, result from insufficient cleaning and/or the particle contamination of the silicon surface. The former is somehow hard to avoid entirely, while the latter can be eliminated completely if the wafer cleaning/transfer processes can be well controlled and optimized. It is more interesting to notice that the IQE response at point C is much lower than that at point B, indicating greater  $J_{sc}$  loss at the cell edge beyond TCO covering. We believe that this observation is because the minority carriers generated in this region need to travel a lateral distance before being collected by TCO, which will increase their possibility of recombination.

To further study this effect, SHJ solar cells with different configurations as shown in Figs. 3(a) and 3(b) are investigated. In configuration A, the TCO layer uncovers the cell edge at the emitter side, while in configuration B, the TCO layer covers the full cell area at the emitter side. For SHJ solar cells with configuration B, the minority carriers generated near the cell edge will go through the i-a-Si:H/p-a-Si:H stack

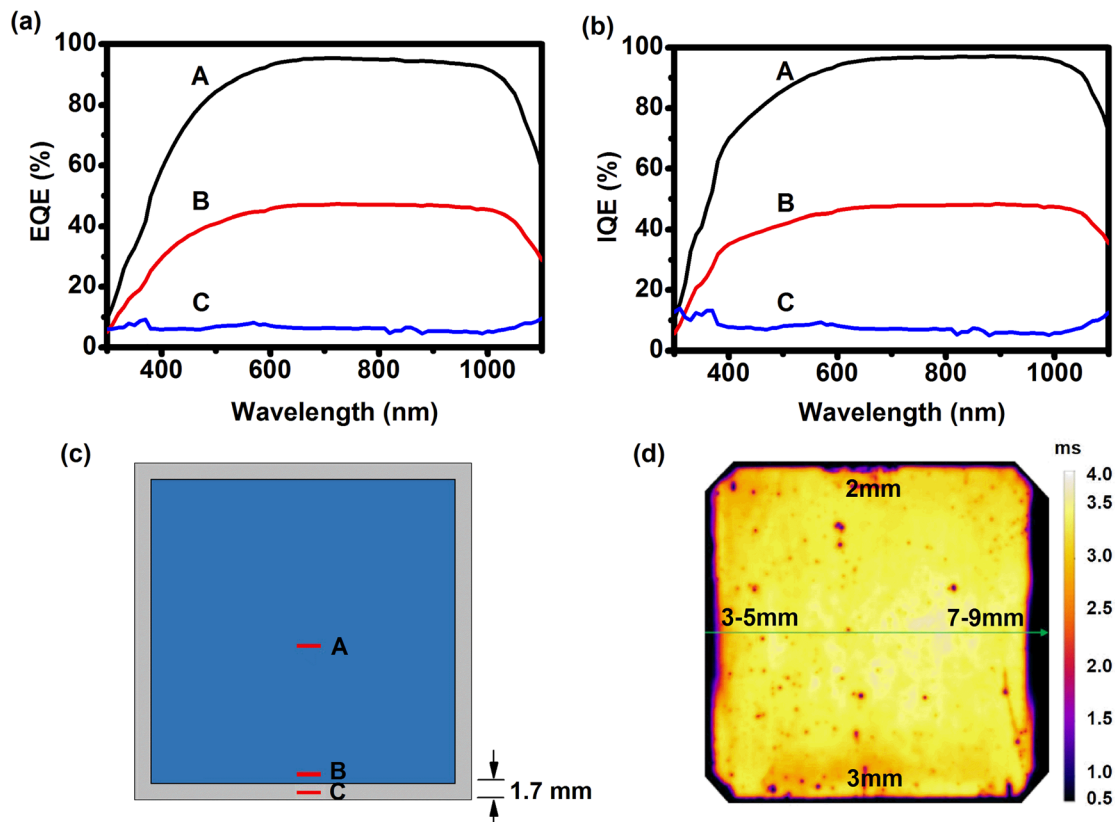


**FIG. 2.** The EQE (a) and IQE (b) responses of the SHJ solar cell detected at the cell center (curves A), the cell edge within TCO covering (curves B) and the cell edge beyond TCO covering (curves C), respectively. (c) Schematic diagram showing the QE detection position (points A, B, and C) corresponding to curves A, B, and C in (a) and (b). (d) The photoluminescence lifetime mapping of the SHJ solar cell without metallization. The widths of the low lifetime area (in black) at four edges are 2 mm, 3–5 mm, 3 mm, and 7–9 mm, respectively.

layer directly and collected by TCO. While for SHJ solar cells with configuration A, the minority carriers generated near the cell edge region beyond TCO covering need undergoing an additional lateral-travel before being collected. As indicated in Fig. 3(a), there may be two possible paths for the minority carriers traveling from the cell edge to the TCO layer. One path is through the inversion layer generated near the interface between the i-a-Si:H/p-a-Si:H stack layer and the c-Si substrate.<sup>16</sup> Another path is through the p-a-Si:H layer. Note that the sheet resistances of the inversion layer<sup>17</sup> and the p-a-Si:H layer are on the order of  $10^3$ – $10^4$   $\Omega/\text{sq}$  and  $10^{10}$   $\Omega/\text{sq}$  (assume that p-a-Si:H has a resistivity of  $10^4$   $\Omega$  cm and a thickness of 10 nm), respectively. It is more likely that the minority carriers will travel through the inversion layer. Figure 3(c) compares the photovoltaic parameters ( $V_{OC}$ ,  $J_{SC}$ ,  $FF$ ,  $Eff$ ,  $R_s$ , and  $R_{sh}$ ) of SHJ solar cells with configurations A and B. It can be found that the average  $J_{SC}$  of SHJ solar cells increases by 0.53  $\text{mA}/\text{cm}^2$  when switching from configuration A to B. This confirms that the additional lateral-travel of the minority carriers before arriving at TCO in configuration A causes heavier recombination, and thus a greater  $J_{SC}$  loss at the edge of the cell. The average  $FF$  of the SHJ solar cells, however, is found to be decreased by 1.6% absolute and results in lower efficiency when switching from configuration A to B. As the series resistances ( $R_s$ ) of the solar cells with configurations A and B are

comparable, the lower  $FF$  of configuration B with an obviously lower shunt resistance ( $R_{sh}$ ) must be caused by edge shunting because the conductivity of n-a-Si:H is much higher than that of p-a-Si:H. To conclude, SHJ solar cells with configuration A suffer from larger  $J_{SC}$  loss caused by edge recombination compared to SHJ solar cells with configuration B. However, SHJ solar cells with configuration A have higher efficiency because they avoid edge shunting effectively.

Based on the above experiments and discussion, we think it is possible to suppress the  $J_{SC}$  loss at the cell edge of configuration A by reducing the gap (D) between the TCO edge and the cell edge [see Fig. 3(a)]. Low D value means a shorter lateral-travel distance that the minority carriers generated at the cell edge need to move before being collected, which means less minority carrier recombination, and thus less  $J_{SC}$  loss. Theoretically speaking, the  $J_{SC}$  of SHJ solar cells with configuration A can be enhanced to the level of configuration B, if D can be set within the diffusion length of the minority carriers (here are holes). Note that the actual mobility value of the inversion layer is lower than the bulk value. Taking the value of hole mobility as  $150 \text{ cm}^2/\text{Vs}$  (Ref. 17) and the value of effective minority carrier lifetime at the cell edge as 0.5 ms [see Fig. 2(d)], the hole diffusion length can be estimated to be 0.4 mm. The experimental results are shown in Fig. 4, and it can be seen that the variation of D leads to the variation of

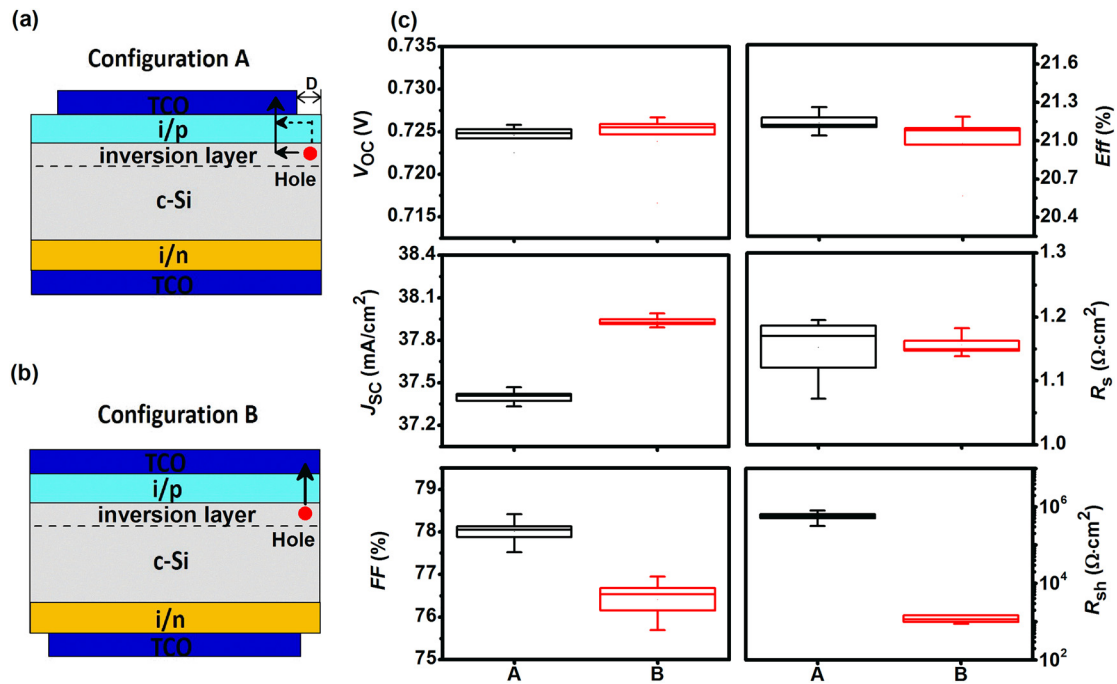


**FIG. 3.** Cross-sectional schematic of SHJ solar cells with configuration A (a) where the TCO layer uncovers the cell edge at the emitter side and configuration B (b) where the TCO layer covers the full cell area on the emitter side. The arrows indicate the possible paths for minority carriers generated near the cell edge region traveling to the TCO layer. D represents the gap between the TCO edge and the cell edge. (c) Comparison of the photovoltaic parameters ( $V_{OC}$ ,  $J_{SC}$ ,  $FF$ ,  $Eff$ ,  $R_s$ , and  $R_{sh}$ ) of the SHJ cells with configurations A and B.

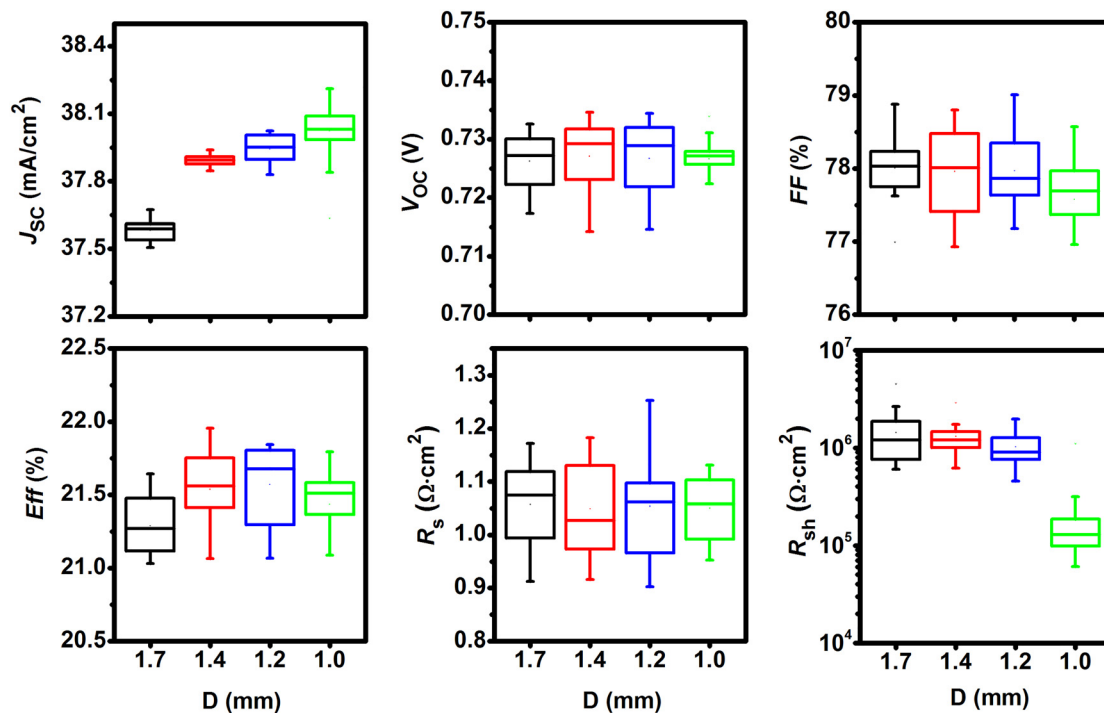


**FIG. 4.** Variation of photovoltaic parameters ( $V_{OC}$ ,  $J_{SC}$ ,  $FF$ ,  $Eff$ ,  $R_s$ , and  $R_{sh}$ ) of the SHJ solar cells with the gap ( $D$ ) between the TCO edge and the cell edge.

$J_{SC}$ ,  $FF$ , and  $R_{sh}$ . As  $D$  decreases from 1.7 mm to 1.2 mm, the average  $FF$  remains stable at around 78.0%, while the average  $J_{SC}$  increases by  $0.36 \text{ mA/cm}^2$  (from  $37.58 \text{ mA/cm}^2$  to  $37.94 \text{ mA/cm}^2$ ), resulting in an average efficiency gain of 0.28% absolute. When  $D$  reduces further to 1.0 mm, the average  $J_{SC}$  gets another increase in  $0.08 \text{ mA/cm}^2$ , while the average  $FF$  drops to 77.6% and cause an average efficiency decrease. This is caused by an obvious  $R_{sh}$  reduction from about  $10^6$  for  $D=1.7\text{--}1.2 \text{ mm}$  to around  $10^5$  for  $D=1.0 \text{ mm}$  due to edge shunting.

#### IV. CONCLUSIONS

In summary, we have demonstrated that the edge recombination effect exists in full area industrial SHJ solar cells, which can cause significant  $J_{SC}$  loss at the cell edge. Furthermore, the  $J_{SC}$  loss is more pronounced at the cell edge region beyond TCO covering, which is because the minority carriers generated in this region need to undergo an additional lateral-travel distance before being collected, thus enhancing their possibility of recombination. We further demonstrate that this  $J_{SC}$  loss effect can be suppressed effectively by reducing the gap between the edge of the TCO layer and that of the cell. The average  $J_{SC}$  of our state-of-the-art SHJ solar cells can be increased by  $0.36 \text{ mA/cm}^2$  without losing  $FF$  and give an average efficiency gain of 0.28% absolute in this way. Overall, trying to improve the edge passivation of the SHJ solar cells is a more fundamental solution for getting rid of the edge recombination problem.

#### ACKNOWLEDGMENTS

This work was supported by the National 863 Program 2011AA050502 and the Program for Innovation and Entrepreneurship of Jiangsu Province.

#### REFERENCES

- <sup>1</sup>K. R. McIntosh, "Lumps, humps and bumps: Three detrimental effects in the current-voltage curve of silicon solar cells," Ph.D. dissertation (University of New South Wales, 2001).
- <sup>2</sup>P. P. Altermatt, G. Heiser, and M. A. Green, "Numerical quantification and minimization of perimeter losses in high-efficiency silicon solar cells," *Prog. Photovoltaics: Res. Appl.* **4**, 355–367 (1996).
- <sup>3</sup>R. Kuhn, P. Fath, and E. Bucher, "Effects of pn-junctions bordering on surfaces investigated by means of 2D-modeling," in *28th IEEE Photovoltaic Specialists Conference* (2000), pp. 116–119.
- <sup>4</sup>A. Fell, J. Schon, M. Muller, N. Wohrle, M. C. Schubert, and S. W. Glunz, "Modeling edge recombination in silicon solar cells," *IEEE J. Photovoltaics* **8**, 428–434 (2018).
- <sup>5</sup>E. Franklin, K. Fong, K. McIntosh, A. Fell, A. Blakers, T. Kho, D. Walter, D. Wang, N. Zin, M. Stocks, E. C. Wang, N. Grant, Y. Wan, Y. Yang, X. L. Zhang, Z. Q. Feng, and P. J. Verlinden, "Design, fabrication and characterisation of a 24.4% efficient interdigitated back contact solar cell," *Prog. Photovoltaics: Res. Appl.* **24**, 411–427 (2016).
- <sup>6</sup>K. C. Fong and S. R. Surve, "Perimeter recombination characterization by luminescence imaging," *IEEE J. Photovoltaics* **6**, 244–251 (2016).
- <sup>7</sup>J. Wong, R. Sridharan, and V. Shanmugam, "Quantifying edge and peripheral recombination losses in industrial silicon solar cells," *IEEE Trans. Electron Devices* **62**, 3750–3755 (2015).
- <sup>8</sup>M. Taguchi, A. Yano, S. Tohoda, K. Matsuyama, Y. Nakamura, T. Nishiwaki, K. Fujita, and E. Maruyama, "24.7% record efficiency HIT solar cell on thin silicon wafer," *IEEE J. Photovoltaics* **4**, 96–99 (2014).
- <sup>9</sup>T. Mishima, M. Taguchi, H. Sakata, and E. Maruyama, "Development status of high-efficiency HIT solar cells," *Sol. Energy Mater. Sol. Cells* **95**, 18–21 (2011).
- <sup>10</sup>C. Battaglia, A. Cuevas, and S. D. Wolf, "High-efficiency crystalline silicon solar cells: Status and perspectives," *Energy Environ. Sci.* **9**, 1552–1576 (2016).
- <sup>11</sup>D. Adachi, J. L. Hernández, and K. Yamamoto, "Impact of carrier recombination on fill factor for large area heterojunction crystalline silicon solar cell with 25.1% efficiency," *Appl. Phys. Lett.* **107**, 233506 (2015).
- <sup>12</sup>M. Kessler, T. Ohrdes, P. P. Altermatt, and R. Brendel, "The effect of sample edge recombination on the averaged injection-dependent carrier lifetime in silicon," *J. Appl. Phys.* **111**, 054508 (2012).
- <sup>13</sup>B. Veith, T. Ohrdes, F. Werner, R. Brendel, P. P. Altermatt, N. P. Harder, and J. Schmidt, "Injection dependence of the effective life time of n-type Si passivated by  $\text{Al}_2\text{O}_3$ : An edge effect?," *Sol. Energy Mater. Sol. Cells* **120**, 436–440 (2014).
- <sup>14</sup>H. Henry, J. Appel, J. Kasthuri, J. Guo, B. Johnson, and J. Binns, "Impact of the injection-level-dependent lifetime on  $V_{oc}$ ,  $FF$ , ideality  $m$ ,  $J_{02}$ , and the dim light response in a commercial PERC cell," *Prog. Photovoltaics: Res. Appl.* **24**, 1448–1457 (2016).
- <sup>15</sup>J. Haschke, O. Dupré, M. Boccard, and C. Ballif, "Silicon heterojunction solar cells: Recent technological development and practical aspects-from lab to industry," *Sol. Energy Mater. Sol. Cells* **187**, 140–153 (2018).
- <sup>16</sup>O. A. Maslova, J. Alvarez, E. V. Gushina, W. Favre, A. S. Gudovskikh, A. V. Ankudinov, E. I. Terukov, and J. P. Kleider, "Observation by conductive-probe atomic force microscopy of strongly inverted surface layers at the hydrogenated amorphous silicon/crystalline silicon heterojunctions," *Appl. Phys. Lett.* **97**, 252110 (2010).
- <sup>17</sup>M. Filipic, Z. C. Holman, F. Smole, S. De Wolf, C. Ballif, and M. Topic, "Analysis of lateral transport through the inversion layer in amorphous silicon/crystalline silicon heterojunction solar cells," *J. Appl. Phys.* **114**, 074504 (2013).